Interface focus

J. R. Soc. Interface (2009) **6**, S715–S726
doi:10.1098/rsif.2009.0311.focus
Published online 7 October 2009

Personalized ventilation as a control measure for airborne transmissible disease spread

Jovan Pantelic[1,*], Gin Nam Sze-To[2], Kwok Wai Tham[1], Christopher Y. H. Chao[2] and Yong Chuan Mike Khoo[3]

[1]*Department of Building, School and Design and Environment, National University of Singapore, Singapore, Singapore*
[2]*Department of Mechanical Engineering, The Hong Kong University of Science and Technology, Kowloon, Hong Kong*
[3]*TSI Instruments, Singapore*

The protective role of personalized ventilation (PV) against plausible airborne transmissible disease was investigated using cough droplets released from a 'coughing machine' simulating the human cough at different distances (1, 1.75 and 3 m) from the PV user. Particle image velocimetry was used to characterize and visualize the interaction between the cough-generated multiphase flow and PV-induced flow in the inhalation zone of the thermal breathing manikin. A dose–response model for unsteady imperfectly mixed environment was used to estimate the reduction in infection risk of two common diseases that can be transmitted by airborne mode. PV was able to both reduce the peak aerosol concentration levels and shorten the exposure time at all the examined injection distances. PV could reduce the infection risks of two diseases, influenza A and tuberculosis, by between 27 and 65 per cent. The protection offered by PV is less effective at a distance of 1.75 m than the other distances, as shown in the risk assessment results, as the PV-generated flow was blown off by the cough-generated flow for the longest time. Results of this study demonstrate the ability of desktop PV to mitigate the infection risk of airborne transmissible disease.

Keywords: airborne infection; transmission; personalized ventilation; cough; breathing thermal manikin; particle image velocimetry

1. INTRODUCTION AND REVIEW OF LITERATURE

Among the sources of indoor pollutants present in the indoor environment, expiratory activities (talking, coughing and sneezing) of infected occupants release pathogen-laden droplets and contribute to the spread of infectious diseases.

Airborne transmission of infectious disease has been defined as the passage of micro-organisms from a source to a person through aerosols, resulting in infection of the person with or without consequent disease (Li *et al.* 2007). Once expiratory droplets are released they start to evaporate at rates dependent on the indoor environmental conditions (with relative humidity (RH), as the most influential) and their initial sizes. Evaporation takes place until the droplet nuclei size is reached, which is defined as the airborne residue of micro-organism-bearing aerosol from which most liquid has evaporated (Wells 1934). Morawska (2006) pointed out several factors in the indoor environment that influence dispersion of expiratory-released droplets: droplet density, number of droplets released, the size distribution of droplets released and airflow patterns generated by the ventilation strategy with respect to source position.

A review by Li *et al.* (2007) concluded that there is sufficiently strong evidence to demonstrate the association between ventilation and the control of airflow directions in buildings and the transmission and spread of infectious diseases such as measles, tuberculosis (TB), chickenpox, anthrax, influenza, smallpox and severe acute respiratory syndrome (SARS). Simulation results from the study of Li *et al.* (2004) on the role of air distribution in SARS transmission indicated that different sizes, positions and number of mixing ventilation (MV) ceiling-mounted supply diffusers and exhaust grilles are capable of reducing bioaerosol concentration by changing the airflow patterns in the hospital ward.

Bolashikov & Melikov (2009) pointed out that the risk of airborne cross-infection can be reduced or increased depending on the airflow patterns generated in the indoor space. Wan & Chao (2005) compared the effects of four different types of supply–exhaust

*Author for correspondence (g0600122@nus.edu.sg).

Electronic supplementary material is available at http://dx.doi.org/10.1098/rsif.2009.0311.focus or via http://rsif.royalsocietypublishing.org.

One contribution of 10 to a Theme Supplement 'Airborne transmission of disease in hospitals'.

Received 23 July 2009
Accepted 7 September 2009

positions on the dispersion of cough-generated droplets and concluded that downward piston-type ventilation flow performed the best in controlling the transmission of cough droplets by reducing the number and lateral dispersion of droplets. These studies indicate that airflow patterns with respect to the position of the source of expiratory droplets (person talking, coughing, sneezing and vomiting) have the most important role in the dispersion of cough droplets in ventilated rooms.

Different technologies have been previously used to clean air of airborne pathogens released in the indoor environment and provide protection to the occupants from infectious disease spread. Dilution based on the increase of supply air flow rate is one of the most frequently used methods for removal of the airborne pathogens. Room air filtration achieves high removal efficiency of droplets with diameters less than 3 μm when the filter is placed close to the occupant, but not for droplets with diameter of less than 1 μm without incorporating a high-efficiency particulate air (HEPA) filter. Ultraviolet (UV) radiation at a wavelength of 254 nm is germicidal and has been used for air disinfection within the indoor environment (Riley 1972). However, this wavelength of UV radiation is irritating to skin and eyes and cannot be used on people; because of this UV lighting is placed at heights between the occupant's head and the ceiling that causes a reduction in the effectiveness of the system. Another important factor influencing the effectiveness of UV lights is indoor RH, which needs to be kept at 50 per cent for optimal performance, whereas at RH levels above 75 per cent the effectiveness is reduced by 40 per cent (Xu *et al.* 2005).

It has been suggested by Melikov (2004) that personalized ventilation (PV) is capable of reducing airborne infectious disease transmission compared with total volume mechanical ventilation.

1.1. Total volume dilution versus dilution in the inhalation zone

A basic principle of ventilation control of pollutants is to direct airflow from the clean zone to the polluted zones (Li *et al.* 2007). Release of expiratory droplets by an infected person is an episodic event in the indoor environment and the source position is largely unknown. Pathogen-laden expiratory droplets in general can move through the indoor environment and spend different amounts of time in different parts of the indoor environment. Total volume ventilation strategies try to address this by dilution of all the air in the indoor volume by supplying greater amounts of clean air to the space through diffusers whose design and position will depend on the ventilation strategy applied.

Instead of diluting the total air volume, the inhalation zone should be kept clean from the pathogen-laden droplets and droplet nuclei by supplying the clean conditioned air at close proximity to the occupant. PV supplying clean air to the breathing zone is able to decrease the inhaled pollutant concentration by factors between 2 and 50 times compared with total-volume ventilation alone (Melikov *et al.* 2002; Cermak *et al.* 2006). Cermak & Melikov (2007) reported that PV in conjunction with underfloor ventilation is more effective in protecting occupants from airborne pathogens released by exhalation than when an underfloor ventilation strategy is applied alone. Owing to the non-uniform environment created by PV, undesirable transport of exhaled pathogens can occur when an infected individual uses PV while the other occupants in the space do not use PV for protection. However, these studies examined particular air terminal device (ATD) designs which create a particular flow field and used gases (e.g. sulphur hexafluoride) to simulate motion of exhaled air as a surrogate for pathogen-laden droplet nuclei. The two-phase flow consisting of suspended cough droplets in the air behaves differently from gas molecules for the same boundary conditions of injection. Droplets are able to maintain higher momentum (velocity) along the pathlines when compared with very rapid momentum (velocity) decay of gas molecules. Droplets and droplet nuclei in the two-phase flow can be deposited onto room surfaces and concentration reduction as deposition cannot be represented with gases. Molecular diffusion can be neglected for cough droplets in air, while for the gases, molecular diffusion is an important transport mechanism; therefore, estimation of cough-droplet dispersion based on sulphur hexafluoride concentration may overestimate the dispersion of cough droplets.

Generally, the equation of aerosol motion contains the Stokes drag, Basset force, fluid pressure gradient force, added mass inertia and gravitational force (Maxey & Riley 1983). Droplets from the mouth are primarily water, hence their density is about 1000 times greater than that of the air phase; therefore the dominant forces acting on the droplets are drag and gravitation forces, all the other forces have much smaller impact on the droplet trajectories and can be neglected in the indoor environment (Burry & Bergeles 1993). Cough droplets with an initial diameter larger than 80 μm tend to settle quickly onto the floor owing to gravity (Chao & Wan 2006), and droplets smaller than 80 μm have the ability to evaporate to droplet nuclei size and a very small response time which enables them to behave as fluid particles. This implies that the flow field generated in the inhalation zone of the occupant is the most important factor influencing protection provided by PV. The flow field generated in the inhalation zone of the occupants consists of complex interactions between several flows: (i) MV generated by the relative supply/return diffuser position, design and flow rate; (ii) buoyancy-driven flow generated by the release of body heat from the occupants; (iii) inhalation/exhalation flow; (iv) PV-generated flow; and (v) cough-generated flow that consists of saliva droplets suspended in the air.

The research objectives in this study are to examine the protective role of desktop personalized ventilation (DPV) combined with MV for mitigation of airborne transmissible disease spread. The protective role was investigated with regards to the cough droplets released from a 'coughing machine' simulating the human cough in a seated position at different distances from the PV user. A dose–response model for an unsteady imperfectly mixed environment was used to estimate the reduction in infection risk of two common diseases that can be transmitted via the airborne mode.

2. MATERIAL AND METHODS

2.1. Experimental facility and equipment

2.1.1. Field experimental chamber. This study was conducted in a field environment chamber (FEC) at the National University of Singapore (figure 1). The FEC has dimensions of 11.12 m (L) × 7.53 m (W) × 2.60 m (H), and the air-conditioning and mechanical ventilation (ACMV) system of the chamber is capable of switching between MV, displacement ventilation and underfloor air-distribution modes. The FEC is also equipped with PV, which is served by its dedicated outdoor air (OA) handling unit and can be used in combination with any of the total volume ACMV systems. Sixteen identical workstations supplied with PV were arranged into four groups of four and symmetrically positioned inside the chamber. For the purpose of the present study three workstations in one of the groups were removed from the FEC in order to facilitate space requirements of the equipment used in this experiment. The single workstation supplied with PV was used for microclimate examination.

2.1.2. Cough machine. A cough machine (Hong Kong University of Science and Technology, Research and Design Corporation Limited, Hong Kong Special Administrative Region, China) was used to simulate multiphase flow consisting of expiratory droplets suspended in the air generated by human cough. Using an air-atomizing nozzle, polydispersed droplets were generated. By fine-tuning the flow rates and pressures of the supply air and liquid to the atomizing nozzle, an expiratory droplet size distribution profile and air-jet velocity similar to human cough can be produced (Wan *et al.* 2007; Sze To *et al.* 2009). The cough machine released puffs of polydispersed droplets simulating human cough. Human saliva was simulated with a mixture of water (94% of the total volume) and glycerin (6% of the total volume). This method of human saliva simulation has been used in several studies (Chao & Wan 2006; Wan *et al.* 2007; Chao *et al.* 2008; Sze To *et al.* 2009). It is also feasible to use this technique in aerosolizing solutions containing benign micro-organisms to simulate pathogen-laden expiratory droplets for a smicrobiological air-sampling study (Sze To *et al.* 2008). In the current study, the nozzle, the flow rates and pressures of the supply air and liquid used in Wan *et al.* (2007) were adopted. These simulate the expiratory droplet size distribution profile reported by Duguid (1946) and the mean cough jet velocity reported by Zhu *et al.* (2006).

2.1.3. Particle image velocimetry. Instantaneous velocity components of the room air flow were captured in a plane by the particle image velocimetry (PIV) technique. Flow seeding was achieved by atomizing olive oil in a TSI 9306 six-jet atomizer (TSI Inc., Shoreview, MN, USA) with an output flow rate of 16.6 l min^{-1} with a mean particle diameter of 0.35 μm and maximum particle diameter of 4 μm (according to the manufacturer's manual). These seeding particles have a response time of the order of 10^{-7} s and

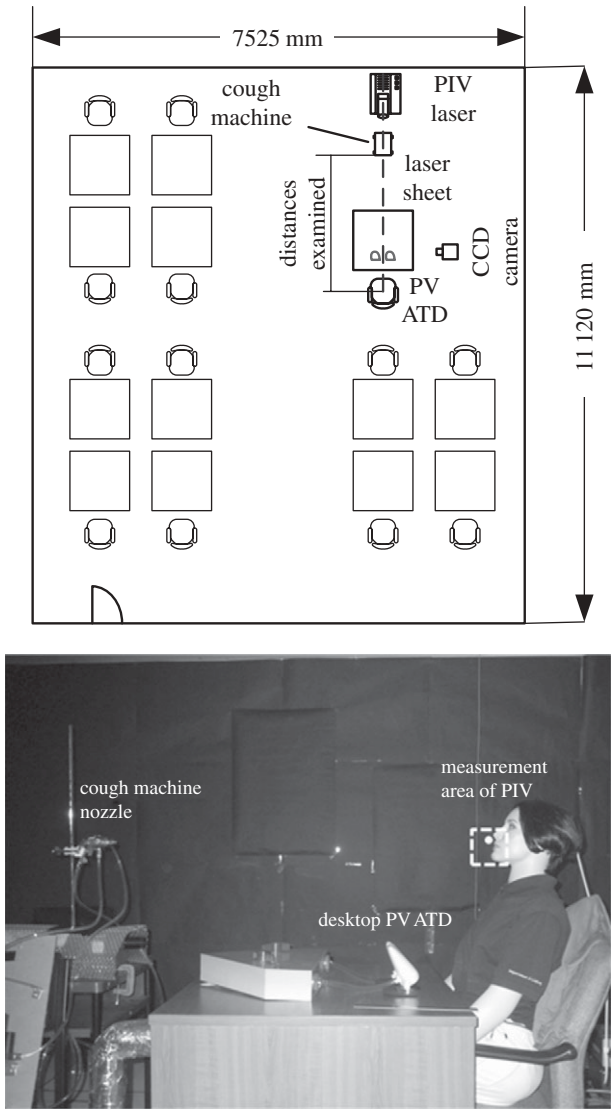

Figure 1. Experimental set-up in a FEC. White dot in front of the manikin's face (inside measurement area of PIV) represents the position of the Grimm 1.108 sampling probe.

represent motion of fluid particles. The PIV system consisted of a dual YAG laser (New Wave Research, Inc., Fremont, CA, USA), double-pulse 190 mJ with a frequency of 15 Hz and a wavelength of 532 nm, light sheet optics, synchronizer, charge-coupled device (CCD) camera (2MP TSI Power View Plus, TSI Inc., Shoreview, MN, USA) and computer. Images captured using the CCD camera were analysed and flow field parameters were computed using Insight 3G software (TSI Inc.). This frequency was well above the characteristic frequencies of the largest eddies found in various types of ventilated spaces (0.04–0.15 Hz) reported by Hanzawa *et al.* (1987). A laser sheet of thickness 1 mm was produced with the laser optics CCD camera positioned orthogonal to the laser sheet with objective lens mounted. The area of each measurement about 150 × 110 mm. Measurements were repeated 10 times in each area.

2.1.4. Aerosol counter. The PIV system allows us to visualize and analyse the interaction between the cough

jet and the PV jet, but to obtain the concentration time profile of the simulated expiratory aerosols, aerosol counting is required. A Grimm 1.108 aerosol spectrometer (Grimm Aerosol Technik GmbH & Co. KG, Germany) with 16 size channels (measurable size range, 0.3–20 μm) is used to measure the real-time aerosol concentration in the inhalation zone of the manikin.

2.1.5. Breathing thermal manikin. To simulate the PV user, a seated breathing thermal manikin (BTM) (P. T. Teknik Limited, Denmark) was used. The manikin is shaped as a 1.68 m tall female, placed in a sitting position. The manikin was dressed in clothing corresponding to approximately 0.7 clo, a typical level of office attire in the tropics. Each of the 26 body segments is heated and individually controlled under the 'comfort mode', which seeks to maintain the manikin's surface temperature equal to the skin temperature of an average human being. With an artificial lung system supplying/sucking the air at a prescribed flow rate, and the nose and mouth shaped as closely as possible to that of the human being, inhalation–exhalation were simulated in terms of frequency, quantity and velocity. To simulate breathing under light office work, the pulmonary ventilation volume was set at $6\,\mathrm{l\,min^{-1}}$, with a 10 times per minute breathing cycle comprising 2.5 s inhalation, 1.0 s break, 2.5 s exhalation and 1.0 s break again, which was similar to that adopted in Zhu *et al.* (2005). The equivalent inhalation–exhalation flow rate was set at $0.24\,\mathrm{l\,s^{-1}}$. The exhaled air was heated to 34°C, but the humidification function was not activated in the present study, because the slight difference in density between humidified and non-humidified air at 34°C was assumed to have negligible impact.

2.2. Experimental design

The cough machine nozzle was positioned at three different distances in front of the manikin: 1, 1.75 and 3 m at a height of 1.15 m from the floor to represent a seated infector. Based on the Centers for Disease Control and Prevention (CDC 2003) guidelines for infection disease transmission, which define large droplet transmission at distances of up to 1 m between the source and susceptible person, and true aerosol transmission occurring at distances larger than 1 m, 1 m was chosen to be the closest distance investigated in the present study.

The influence of two different ventilation strategies was examined in this study: (i) ceiling supply MV and (ii) combination of PV and ceiling supply MV. Two DPV ATDs were used in this study to supply the outdoor conditioned air to the manikin in scenario (ii). They were positioned on the surface of the desk 250 mm from the manikin's nose. PV ATDs were also pivoted in such a way that they supplied the OA towards the inhalation zone (nose) of the manikin.

A PIV laser-generated sheet was aligned with the centreline of the BTM, and the CCD camera was positioned orthogonal to the laser sheet. During the PIV measurement, part of the manikin's face was covered with black paper to reduce the CCD camera exposure to laser light which was reflected from the curvature of the manikin's face and could possibly cause damage to the CCD camera (figure 1). The flow field was divided into several measurement areas and a series of images were taken in each measurement area.

Measurement of the number of droplets in the inhalation zone of the manikin was conducted with a Grimm 1.108 spectrometer. The isokinetic probe was positioned 15 mm below the manikin's nose and 15 mm from the manikin's upper lip (indicated as a dot in figure 1). The droplet number concentration was measured at 1 s intervals. Measurements were performed with the manikin set in two modes: breathing and non-breathing. The average aerosol count in the first 10 s before the injection of droplets was taken as the background particle level, which was subsequently deducted from the droplet number concentration data collected after the cough droplets injection. Every measurement was conducted for 60 s because, from real-time aerosol concentration monitoring, it was found that 60 s is sufficient for the concentration level to drop back to the background level in all relevant scenarios. Ten repeat measurements were taken at each distance (1, 1.75, 3 m) setting.

Room air temperature was maintained at 23°C with ceiling supply/return MV. The supply flow rate by MV achieved six air changes per hour in a room. PV conditioned air consisted of 100 per cent OA and was supplied at a total flow rate of $5\,\mathrm{l\,s^{-1}}$ ($2.5\,\mathrm{l\,s^{-1}}$ for each ATD) at a temperature of 23°C. Relative humidity in the room was maintained below 60 per cent. These conditions achieved steady state before puffs of cough droplets were released. Once cough droplets were released, they created unsteady state conditions in the indoor environment. When the conditions created by the cough puffs decayed, conditions in the experimental chamber returned to the steady state.

The method suggested by Nicas *et al.* (2005) was used to calculate the time required for droplets to evaporate from initial to droplet nuclei size. The droplets with an initial diameter of 50 μm evaporated to a droplet nuclei size of 20 μm (the largest droplet size that can be sampled with the Grimm 1.108 spectrometer) in 1.74 s. For the smaller droplets, for example with initial size of 12 μm (the largest number of droplets released by the cough machine was in this size), 0.1 s was required for the droplets to reach droplet nuclei size. When the cough machine was positioned at 1.75 m from the thermal manikin, droplets reached the inhalation zone in approximately 1.5 s. After comparing evaporation time and the time necessary for the droplets to reach the inhalation zone after injection, we believe it is reasonable to assume that evaporation was instantaneous.

2.3. Infection risk assessment

To demonstrate how the infection risk is reduced, infection risk assessment was performed. Infection risk assessment is a useful tool in studying disease transmission and evaluating the effectiveness of infection control measures.

The infection risk of an individual or a population to an infectious disease is expressed by a probability of

infection between 0 and 1. Infection risk assessment consists of the estimation of the intake dose of the infectious agent and the estimation of the probability of infection under the given intake dose. Estimation of intake dose requires knowing the exposure level to the infectious agent, the duration of exposure and the intake rate. Knowing the intake dose, the probability of infection can then be modelled by a mathematical function that describes the dose–infection relationship (Haas *et al.* 1999).

The exposure level to airborne pathogen can be estimated by directly counting the concentration time profile of the expiratory aerosols in the inhalation zone combined with the viability characteristic of the airborne pathogen (Sze To *et al.* 2008)

$$E(t_0) = \theta t_0 cp \int_0^{t_0} v(t) f\,(t) \mathrm{d}t, \tag{2.1}$$

where $E(t_0)$ is the exposure level of the susceptible person to the pathogen during the exposure time interval, t_0, θ the cough frequency of the infector, c the pathogen concentration in the respiratory fluid, p the pulmonary ventilation rate of a person, $f(t)$ the viability function of the virus in the aerosols, and $v(t)$ the volume density of expiratory droplets at the inhalation zone after the infector produces a single cough.

When airborne pathogens are inhaled by the receptor organism, a fraction of the inhaled pathogen-laden aerosols may deposit on the target infection site in the respiratory tract. This respiratory deposition of infectious particles is dependent on their sizes. Owing to aerosol size dependency of the respiratory deposition, the aerosols have different deposition fractions on different regions in the respiratory tract. For example, aerosols with sizes $>6\,\mu$m are trapped increasingly in the upper respiratory tract, aerosols with sizes $>20\,\mu$m are generally not deposited in the lower respiratory tract, and those with sizes $>10\,\mu$m generally do not reach the alveolar region (Hinds 1999; Tellier 2006).

In addition, pathogens generally have different infectivity in different regions of the respiratory tract owing to different immune mechanisms in different regions of the respiratory tract. For example, the ID_{50} (a dose of the pathogen that causes a 50% infection rate) of influenza virus is about two orders higher when the virus is introduced to the nasal cavity by intranasal drop than when it is introduced to the lower respiratory tract via aerosol inhalation (Alford *et al.* 1966; Douglas 1975). Since respiratory deposition of aerosols depends on their sizes, the variation in pathogen infectivity when carried by infectious particles of different sizes was also observed, as shown by many experimental infection studies (e.g. Wells 1955; Day & Berendt 1972). To consider these factors, the exposure level should be divided into different size bins in the risk assessment model (Sze To *et al.* 2008)

$$P_{\mathrm{I}}(t_0) = 1 - \exp\left(\sum_{j=1}^{m} r_j \beta_j \theta t_0 cp \int_0^{t_0} v(t)_j f\,(t) \mathrm{d}t\right), \tag{2.2}$$

where $P_{\mathrm{I}}(t_0)$ is the probability of infection of the susceptible person, m the total number of size bins, $v(t)_j$ the volume density of droplets of the jth size bin, and β the deposition fraction of the infectious particle. Equation (2.2) is an exponential dose–response model. The infectivity term of the pathogen, r, is calculated using infectious dose data; for example, with ID_{50} data, r can be calculated as $-\ln 0.5/ID_{50}$. If data on more than one infectious dose are available, r should be obtained from maximum likelihood fitting (Haas *et al.* 1999).

The aerosol counting data in the inhalation zone of the manikin are used to obtain $v(t)_j$. Most expiratory droplets will evaporate and shrink to their droplet nuclei sizes within a second (Wan *et al.* 2007; Xie *et al.* 2007). The measured aerosol sizes are droplet nucleus sizes. The measured nucleus sizes were back-adjusted to their initial droplet sizes to calculate $v(t)_j$ (Sze To *et al.* 2008), since c in equation (2.1) refers to the pathogen concentration in the human respiratory fluid before aerosolization. The nucleus sizes of the aerosols are adopted for β_j and r_j, since they are the inhaled particle sizes. Infection risk assessments of a sitting person at different injection distances with and without PV protection were performed using equation (2.2).

The ability of the PV to provide protection by reducing the infection risk was then evaluated. The infection risk of two diseases, tuberculosis and influenza A, was assessed. Influenza A viruses are nanometre scale biological particles that can infect both the upper and lower respiratory tracts. Tuberculosis bacilli are bacterial cells of sizes ranging from 1 to 4 μm (Cole & Cook 1998) and infect only the alveolar region. Since particles with sizes $>10\,\mu$m generally do not reach the alveolar region and droplets with sizes $<1\,\mu$m will not contain the bacillus, aerosols with nuclei sizes $>10\,\mu$m and droplet sizes $<1\,\mu$m were excluded in calculating the infection risk for tuberculosis. The epidemiological data used in the infection risk assessment are shown in table 1. An exposure time interval of 8 h was used in all scenarios.

3. RESULTS AND DISCUSSION

Results are presented from the measurement area (indicated in figure 1), which contained the inhalation zone of the manikin as well as the zone in which the cough machine-generated flow interacted with the DPV-induced flow field, buoyancy-driven flow and inhalation–exhalation flow. Owing to different light-scattering properties of simulated saliva droplets and olive oil seeding in the PV flow, PIV images can be used to distinguish these two flows and visualize their interaction. Details are shown in figure 2*a*,*b* for the cough scenario at the 1.75 m distance. Owing to space limitations, only images from this scenario are depicted here. The images in the electronic supplementary material depict the velocity profiles of the cough droplets and the PV-generated flow for the scenarios at the 1 m and 3 m distances.

3.1. Cough distance 1 m

The initial puff velocity produced by the cough machine was about 10 m s^{-1} and the flow field generated had a strong enough momentum to fully blow away the DPV flow field created around the manikin's face.

Table 1. Epidemiological data used for infection risk assessment. c, the pathogen concentration in the respiratory fluid; $TCID_{50}$, 50% tissue culture infectious dose, a unit used to describe the quantity of virus; cfu, colony–forming unit, a unit used to describe the quantity of bacterial cells; β, deposition fraction of the infectious particle; θ, cough frequency of the infector; r, infectivity term of the pathogen, which can be calculated using infectious dose data, e.g. with ID_{50} data, r can be calculated as $-\ln 0.5/ID_{50}$; $f(t)$, viability time function of the pathogen, t has the unit of hours.

parameter	influenza A	remarks	tuberculosis	remarks
c	5×10^5 $TCID_{50}$ ml^{-1}	median concentration from 7 patients (Murphy *et al.* 1973)	7×10^4 cfu ml^{-1}	mean concentration of bacillus in saliva (Yeager *et al.* 1967)
human infectious dose and respiratory deposition	$ID_{50} = 1.8$ $TCID_{50}$ $r = 0.385$	infectious dose for aerosols$\leq$3 μm, mean value of the range: 0.6–3.0; $\beta = 0.6$ (Alford *et al.* 1966)	$r = 1$ (Jones *et al.* 2009)	a single bacillus is sufficient to cause infection (Wells 1955)
	$ID_{50} = 223.5$ $TCID_{50}$ $r = 0.0031$	upper respiratory tract infectious dose, for larger aerosols, mean value of the range: 127–320 reported by Douglas (1975); β, total respiratory fraction reported by Hinds (1999).		β, human alveolar deposition fraction reported by Asgharian *et al.* (1995).
airborne viability	8% once aerosolization, down to 7% after 15 min $f(t) = 0.08e^{-0.53t}$	extrapolated from fig. 2*b* in Schaffer *et al.* (1976), room temperature, 60% RH	13.7% once aerosolization, down to 9% after 3 h $f(t) = 0.137e^{-0.14t}$	average of two trials reported by Loudon *et al.* (1969), 21°C, approx. 50% RH
θ	18 cough h^{-1}	median cough frequency of 60 patients (Loudon & Brown 1967)	82 cough h^{-1}	median cough frequency of 96 pulmonary tuberculosis patients (Loudon & Brown 1967)

Decay of the velocity of the cough droplets was not sharp owing to the short distance between the cough machine nozzle and manikin, and when the droplets reached the measurement area in which they interacted with PV-generated flow cough droplet velocity was in the range of 2.5–3.5 m s^{-1}. Although the cough jet was initially very strong and had the ability to instantly blow off PV-generated flow field, velocity decay in the same measurement region was very fast once droplets had passed through the measurement area. After 0.06 s, the velocity of the droplets reduced from 2.5–3.5 m s^{-1} to 1.5–2.5 m s^{-1} (see electronic supplementary material, figures S1 and S2).

The average aerosol concentration time profiles from 10 trials at three different distances with and without PV are shown in figure 3. Measurement of the number concentration of droplets indicates that after high peak value was reached the concentration reduced rapidly and reached background level in a few seconds.

This velocity decay and rapid decay in the droplet number concentration indicate that droplets move as a bulk and are not highly dispersed before reaching the manikin's face. The peak value of the number concentration occurred during the period when the PV-generated flow field was completely blown off. Rapid decay of cough droplet velocity in the inhalation zone of the manikin enabled DPV-generated flow to re-establish itself in the inhalation zone of the manikin after 0.48 s from the moment it was blown away (see electronic supplementary material, figures S1 and S2). This re-establishment enabled the PV-generated flow field to bring clean air to the inhalation zone and rapidly reduce the concentration of the droplets. Comparison of the droplet number concentration measured in the inhalation zone between MV and PV combined with the MV scenarios indicates that significantly faster decay to the room background level was achieved when PV and MV were used together (figure 3).

3.2. Cough distance 1.75 m

Although the droplets were more dispersed than in the previous case (distance at 1 m), the multiphase flow generated by the cough machine still had sufficient momentum to blow away the PV-generated flow, which was re-established after 1.1 s. Maximum velocity reached in the measurement area was 2 m s^{-1}. The time period without PV-generated flow in the inhalation zone (1.1 s) was longer than in the 1 m case and thus prolonged the time when the droplet number concentration in the inhalation zone was dominantly influenced by the cough-generated flow field. In other words, the time period without the protection of PV-generated flow was longer than that in the 1 m case. After 1.1 s from the moment it was blown off, the cough flow loses its momentum and DPV-generated flow was able to re-establish itself again (figures 2 and 4).

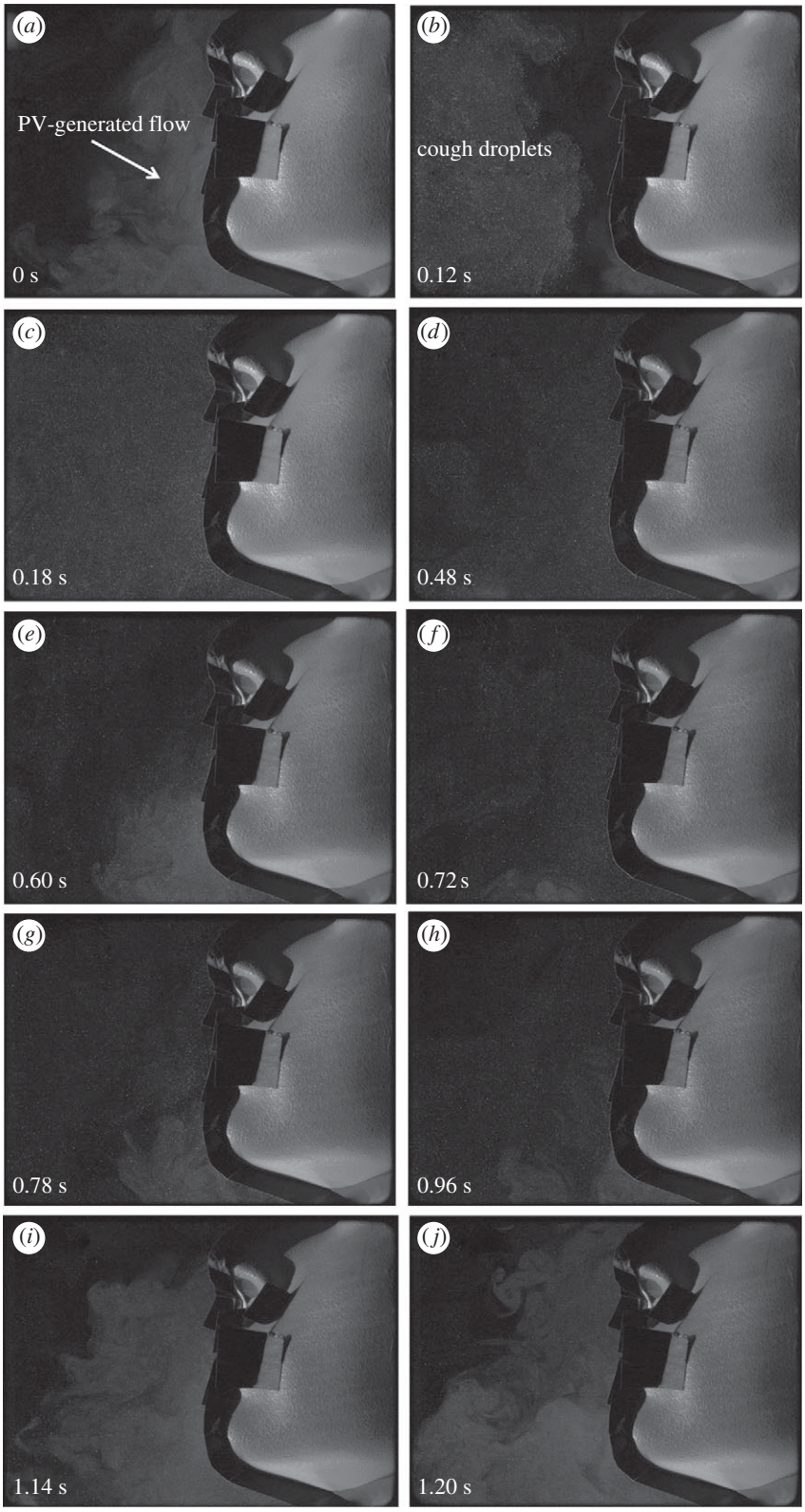

Figure 2. Interaction of the cough machine flow field and PV flow field at the 1.75 m distance case. Time shown in the bottom left corner of (*a*) shows conditions around 1.3 s after injection. (*a*) PV flow only; (*b*) cough droplets are coming and blowing off PV flow; (*c*–*h*) cough machine-dominated flow in the inhalation zone totally disabling PV to fully re-establish itself with some periodical penetration in the bottom part of the figures; (*i*, *j*) re-establishment of PV flow.

After the re-establishment of DPV flow in the inhalation zone, purging of the droplets in the inhalation zone starts, which resulted in a rapid reduction in the cough droplet number concentration (figure 3).

3.3. Cough distance 3 m

When the cough-generated flow field reached the inhalation zone of the manikin, the droplets were more dispersed than in the previous two cases and had less

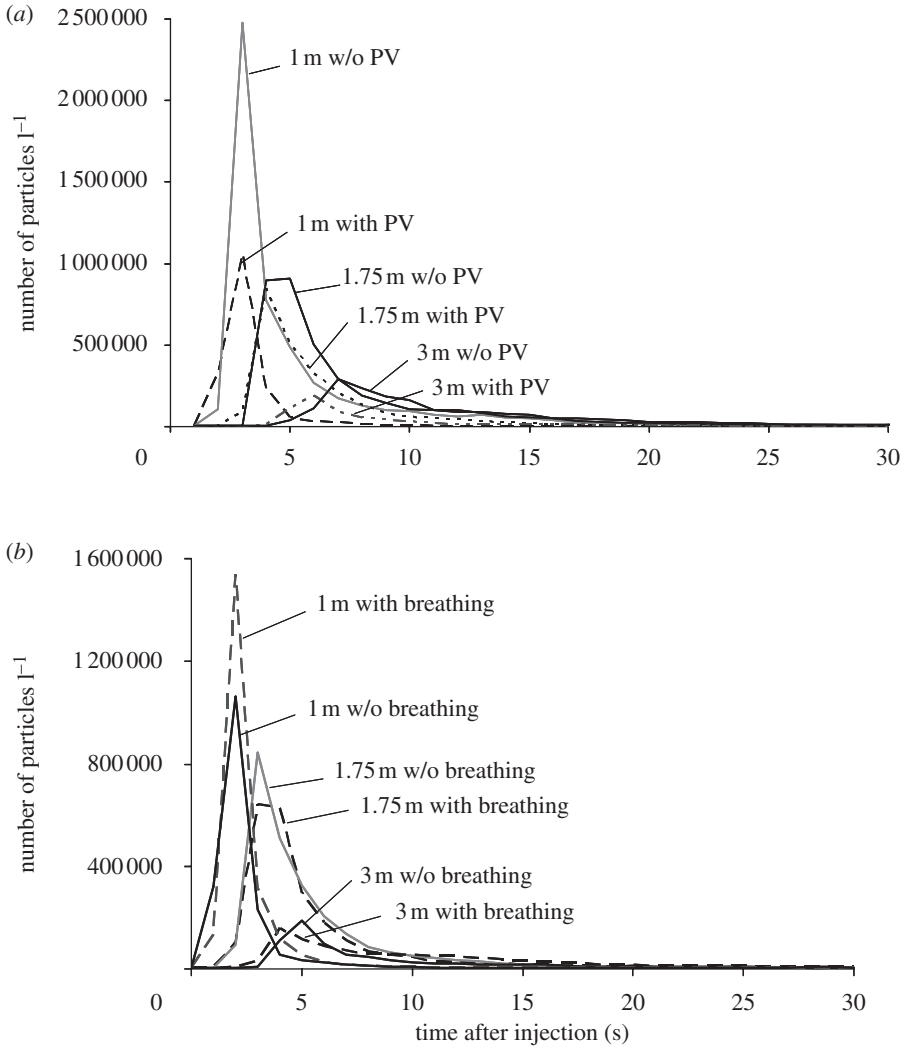

Figure 3. Average aerosol concentration time profiles from 10 trials at three different distances with and without (w/o) personalized ventilation. (*a*) The breathing function of the manikin was disabled during this set of measurements. (*b*) The aerosol concentration time profiles with personalized ventilation. The breathing function of the manikin has no significant effect on these measurements.

momentum. The velocity of cough droplets in the measurement area was less than 1 m s^{-1}. The PV flow field was able to dominate the flow in the inhalation zone of the manikin. In some trials in this case, the cough multiphase flow was able to blow off the DPV flow but only for a period of around 0.06 s, after which the DPV flow re-established itself and purged the inhalation zone of the manikin. At this distance, the droplets were even more dispersed than in the 1.75 m case (see electronic supplementary material, figures S4 and S5).

Therefore, the reduction in aerosol concentration to the background level took an even longer period of time (figure 3) and had a more significant fluctuation of the droplet concentration. This increased the time necessary for the measured aerosol concentration to reach the room background level when compared with the other distances, but with a much lower peak concentration level owing to the always present PV flow, which was able to remove the droplets from the inhalation zone.

3.4. Improved purging of aerosols in the inhalation zone

The peak count and time required to reduce the droplet number concentration to the background level at three different distances with and without PV are summarized in table 2. Since theoretically it will take an infinitely long time for the aerosol concentration to fall back to the background level, the purging time is defined as the time required for the aerosol count to drop from the peak count level to 1.2 times the background level. PV is able to reduce both the peak count and the purging time and hence reduce the exposure level of the person to the expiratory droplets. The effect of breathing on the aerosol concentration time profiles is not significant, as shown in figure 3*b*. In table 2, the peak count levels are generally similar when breathing is enabled and when breathing is disabled. The times required to reduce the aerosol number concentration to the background level are also similar in general. This suggests that the periodic

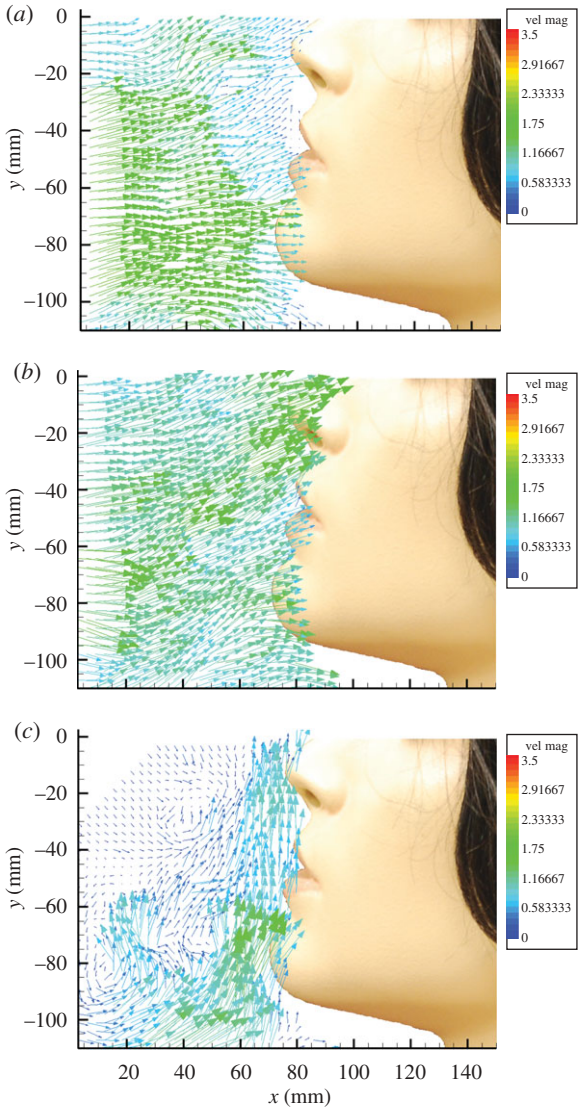

Figure 4. PIV measured vector field of the initial blow off of the PV-generated flow at 1.75 m distance; (*a*) is the vector field calculated using the image in figure 2*b*; (*b*) is the vector field calculated by PIV software using the image in figure 2*c*; and (*c*) is the vector field calculated by PIV software using the image in figure 2*j*.

breathing air pattern at the inhalation zone will not significantly affect the exposure level. Tables 3 and 4 show the statistics of exposure levels calculated from the 10 measurements under all the examined scenarios. The differences in exposure levels with and without breathing were not significant among all the cases examined. Statistical significance test (*t*-test) was performed to compare the exposure levels among cases with PV and those without PV. All the *t*-values are greater than the critical *t*-value for a 95 per cent confidence interval, indicating that the reduction in exposure by the PV device is statistically significant in all the examined scenarios.

3.5. Reduction of infection risk

Infection risk assessments of influenza A and tuberculosis based on real epidemiological data are shown in figure 5. The mean intake dose value is used in the risk calculation instead of the intake dose value based on a single trial. Since equation (2.2) has already incorporated the variability of the intake dose using the Poisson probability concept (Haas *et al.* 1999), a mean value should be used in the equation.

From the results, PV protection has the potential to reduce the infection risks of both diseases in all scenarios. It was also found that the effect of breathing plays an insignificant role in the risk levels. It is intuitively expected that the shorter the distance between the infectious source and the susceptible person, the greater the infection risk to the susceptible person, but at a distance of 1.75 m with PV, the risks are slightly higher than in the 1 m distance cases.

At a distance of 1.75 m, the cough flow was able to blow away PV flow for the longest period (1.1 s) among all examined cases, and therefore PV offered the least protection in this case. Even so, PV is still able to reduce the infection risk at this distance. The percentage reduction of infection risk is summarized in table 5.

The potential percentage reduction of infection risk of tuberculosis is greater than that of influenza A at all distances. This is due to the nonlinearity of the dose–infection relationship. Having the same percentage reduction in exposure level would mean that infection risk reduction will be more significant in a lower risk level than in a higher risk level. Tuberculosis has lower risk levels than influenza A in the scenarios studied, thus the reduction of risk levels is more significant under the same control measure.

For both diseases, the percentage reductions at 1 m and 3 m distances are similar, while the percentage reduction at the 1.75 m distance is not as efficient as the other two. This shows that the protection in the 1.75 m case is the least among all the three distances examined in this study. The infection risk reduction suggests that the PV protection technology is able to mitigate the spread of airborne transmissible diseases significantly. PV can significantly reduce the risk levels even as close as 1 m distance, suggesting that the technology is also able to offer protection to the user in close proximity to the infectious source.

The current global pandemic of influenza A H1N1 flu reiterates the rapid spreading of airborne transmissible diseases in the world. Some studies estimate that aerosol transmission of influenza virus is more dominant than other transmission pathways (Atkinson & Wein 2008; Wan *et al.* 2009), while another study estimates that contact or droplet transmission is the most dominant pathway (Nicas & Jones 2009). The difference in their conclusions could be due to the difference in conditions used in the risk assessment. This also suggests that under different scenarios transmission pathways other than the airborne route are also important. Nevertheless, airborne transmission is still an important concern in the spreading of influenza as well as other respiratory infectious diseases. The current results demonstrate that PV is able to offer some protection against this transmission pathway.

Table 2. Reduction in peak aerosol count and purging time under personalized ventilation protection. PV, personalized ventilation. Background count levels are extracted in the peak count values. The peak count, purging time and the reduction are mean values of the 10 trials.

	without PV		with PV		reduction	
distance (m)	peak count (particles l^{-1})	purging time (s)	peak count (particles l^{-1})	purging time (s)	peak count (%)	purging time (%)
	without breathing					
1.0	2 479 936	17.8	1 062 199	6.0	57	66
1.75	907 443	18.3	844 125	15.6	7	15
3.0	293 615	27.9	188 352	20.1	36	28
	with breathing					
1.0	2 059 592	15.8	1 538 266	7.5	25	52
1.75	835 460	22.4	645 306	15.0	23	33
3.0	290 412	20.0	159 744	19.3	45	3.5

Table 3. The mean, s.d. and range of exposure levels to the expiratory aerosols calculated from the 10 measurements. Note: 0.0075 ml of simulated saliva was injected into the air in each measurement.

	without PV			with PV		
distance (m)	mean exposure level (ml)	s.d. (ml)	range (ml)	mean exposure level (ml)	s.d. (ml)	range (ml)
	without breathing					
1.0	1.85×10^{-4}	3.18×10^{-5}	1.35×10^{-4} – 2.31×10^{-4}	6.12×10^{-5}	1.15×10^{-5}	3.93×10^{-5} – 7.61×10^{-5}
1.75	1.21×10^{-4}	2.85×10^{-5}	8.03×10^{-5} – 1.61×10^{-4}	7.43×10^{-5}	1.38×10^{-5}	5.55×10^{-5} – 9.83×10^{-5}
3.0	6.77×10^{-5}	1.64×10^{-5}	3.62×10^{-5} – 9.37×10^{-5}	2.46×10^{-5}	9.18×10^{-6}	8.87×10^{-6} – 3.83×10^{-5}
	with breathing					
1.0	1.82×10^{-4}	2.90×10^{-5}	1.38×10^{-4} – 2.41×10^{-4}	6.14×10^{-5}	1.30×10^{-5}	3.75×10^{-5} – 8.08×10^{-5}
1.75	1.21×10^{-4}	2.29×10^{-5}	8.51×10^{-5} – 1.53×10^{-4}	6.85×10^{-5}	9.06×10^{-6}	5.61×10^{-5} – 8.31×10^{-5}
3.0	6.02×10^{-5}	1.63×10^{-5}	2.90×10^{-5} – 8.55×10^{-5}	3.13×10^{-5}	9.52×10^{-6}	1.99×10^{-5} – 4.76×10^{-5}

Table 4. Results of statistical significance test (*t*-test) on the reduction of exposure level by PV. Critical *t*-value for 95 per cent confidence interval is 2.10.

distance (m)	*t*-value	*p*-value
	without breathing	
1.0	11.51	$<1 \times 10^{-6}$
1.75	4.70	top of form 0.000179
3.0	7.25	top of form 0.000001
	with breathing	
1.0	11.95	$<1 \times 10^{-6}$
1.75	6.80	top of form 0.000002
3.0	4.86	top of form 0.000127

4. SUMMARY

The following conclusions can be drawn from the above discussion:

(i) The droplets that were released by the cough machine at a distance of 1 m from the manikin move in bulk and had high velocity when they reach the inhalation zone. This momentum was able to blow away PV flow created in the inhalation zone of the manikin. When PV flow was blown off, the number of cough droplets in the inhalation zone reached maximum value, but since droplets move away from the inhalation region very fast, PV flow was able to re-establish itself quickly and rapidly reduce the concentration of the droplets in the inhalation zone.

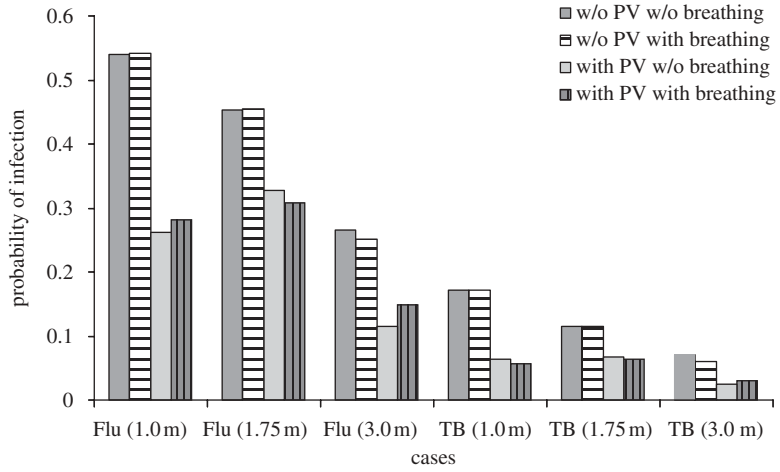

Figure 5. Infection risk assessment result. Flu, influenza A; TB, tuberculosis. The mean intake doses calculated from the 10 trials are used. A t_0 of 8 h was used for the assessment.

Table 5. Percentage reduction in infection risk by personalized ventilation protection.

	reduction (%)	
distance (m)	influenza A	tuberculosis
1.0	51.3	63.0
1.75	27.7	41.4
3.0	54.5	64.6

(ii) Interaction observed in the 1.75 m case implied that redistribution of momentum in the multiphase flow generated by the cough machine due to dispersion has an important influence on the time that will be needed for DPV flow to re-establish itself in the inhalation zone. Hence this interaction has a strong influence on the exposure and protection achieved by PV, which was the least among all the cases examined in this study.

(iii) At the 3 m distance the cough-generated multiphase flow was not strong enough to blow away the PV-generated flow.

(iv) PV was able to both reduce the peak aerosol concentration levels and shorten the exposure time at all the examined injection distances. PV could reduce the infection risks of two diseases, influenza A and tuberculosis, by between 27 and 65 per cent. It was also found that the effect of breathing has an insignificant effect on the risk levels. The protection offered by the PV is least effective at a distance of 1.75 m compared with the other distances, as shown in the risk assessment results, as the PV-generated flow was blown off by the cough-generated flow for the longest time.

(v) PV can significantly reduce the risk levels even as close as 1 m; this suggests that the technology is also able to offer protection to the user even in close proximity to the infectious source.

The results of this study therefore demonstrate the potential ability of DPV ATD to mitigate the infection risk of airborne transmissible disease.

The financial support of the National University of Singapore (NUS) through Research Project grant R296-000-126-112 and from the Hong Kong Research Grant Council via GRF grant 611506 is gratefully acknowledged.

REFERENCES

Alford, R. H., Kasel, J. A., Gerone, P. J. & Knight, V. 1966 Human influenza resulting from aerosol inhalation. *Proc. Soc. Exp. Biol. Med.* **122**, 800–804.

Asgharian, B., Wood, R. & Schlesinger, B. 1995 Empirical modeling of particle deposition in the alveolar region of the lungs: a basis for interspecies extrapolation. *Fundam. Appl. Toxicol.* **27**, 232–238. (doi:10.1006/faat.1995.1128)

Atkinson, M. P. & Wein, L. M. 2008 Quantifying the routes of transmission for pandemic influenza. *Bull. Math. Biol.* **70**, 820–867. (doi:10.1007/s11538-007-9281-2)

Bolashikov, Z. D. & Melikov, A. K. 2009 Methods for air cleaning and protection of building occupants from airborne pathogens. *Build. Environ.* **44**, 1378–1385. (doi:10.1016/j.buildenv.2008.09.001)

Burry, D. & Bergeles, G. 1993 Dispersion of particles in anisotropic turbulence. *Int. J. Multiphase Flow* **19**, 651–664. (doi:10.1016/0301-9322(93)90093-A)

CDC 2003 *Guidelines for environmental infection control in health-care facilities*. Atlanta, GA: Centers for Disease Control and Prevention.

Cermak, R. & Melikov, A. K. 2007 Protection of occupants from exhaled infectious agents and floor material emissions in rooms with personalized and underfloor ventilation. *HVAC&R Res.* **13**, 23–38.

Cermak, R., Melikov, A. K., Forejt, L. & Kovar, O. 2006 Performance of personalized ventilation in conjunction with mixing and displacement ventilation. *HVAC&R Res.* **12**, 295–311.

Chao, C. Y. H. & Wan, M. P. 2006 A study of the dispersion of expiratory aerosols in unidirectional downward and ceiling-return type air flows using multiphase approach. *Indoor Air* **16**, 296–312. (doi:10.1111/j.1600-0668.2006.00426.x)

Chao, C. Y. H., Wan, M. P. & Sze To, G. N. 2008 Transport and removal of expiratory droplets in hospital ward environment. *Aerosol Sci. Technol.* **42**, 377–394.

Cole, E. C. & Cook, C. E. 1998 Characterization of infectious aerosols in health care facilities: an aid to effective engineering controls and preventive strategies. *Am. J. Infect. Control* **26**, 453–464. (doi:10.1016/S0196-6553(98)70046-X)

Day, W. C. & Berendt, R. F. 1972 Experimental tularemia in *Macaca mulatta*: relationship of aerosol particle size to the infectivity of airborne pasteurella tularensis. *Infect. Immun.* **5**, 77–82.

Douglas, R. G. 1975 Influenza in man. In *The influenza viruses and influenza* (ed. E. D. Kilbourne), pp. 375–447. New York, NY: Academic Press.

Duguid, J. 1946 The size and duration of air-carriage of respiratory droplets and droplet nuclei. *J. Hyg.* **4**, 471–480.

Haas, C. N., Rose, J. B. & Gerba, C. P. 1999 *Quantitative microbial risk assessment*. New York, NY: John Wiley & Sons, Inc.

Hanzawa, H., Melikow, A. K. & Fanger, P. O. 1987 Airflow characteristics in the occupied zone of ventilated spaces. *ASHRAE Trans.* **93**, 524–539.

Hinds, W. C. 1999 *Aerosol technology*. New York, NY: John Wiley & Sons, Inc.

Jones, R. M., Masago, Y., Bartrand, T., Haas, C. N., Nicas, M. & Rose, J. B. 2009 Characterizing the risk of infection from mycobacterium tuberculosis in commercial passenger aircraft using quantitative microbial risk assessment. *Risk Anal.* **29**, 355–365. (doi:10.1111/j.1539-6924.2008.01161.x)

Li, Y., Huang, X., Yu, I. T. S., Wong, T. W. & Qian, H. 2004 Role of air distribution in SARS transmission during the largest nosocomial outbreak in Hong Kong. *Indoor Air* **15**, 83–95. (doi:10.1111/j.1600-0668.2004.00317.x)

Li, Y. *et al.* 2007 Role of ventilation in airborne transmission of infectious agents in the built environment—a multidisciplinary systematic review. *Indoor Air* **17**, 2–18. (doi:10.1111/j.1600-0668.2006.00445.x)

Loudon, R. G. & Brown, L. C. 1967 Cough frequency in patients with respiratory disease. *Am. Rev. Resp. Dis.* **96**, 1137–1143.

Loudon, R. G., Bumgarner, L. R., Lacy, J. & Coffman, G. K. 1969 Aerial transmission of mycobacteria. *Am. Rev. Resp. Dis.* **100**, 165–171.

Maxey, M. R. & Riley, J. J. 1983 Equation of motion for a small rigid sphere in a nonuniform flow. *Phys. Fluids* **26**, 883–889. (doi:10.1063/1.864230)

Melikov, A. K. 2004 Personalized ventilation. *Indoor Air* **14**(Suppl. 7), 157–167.

Melikov, A. K., Cermak, R. & Majer, M. 2002 Personalized ventilation: evaluation of different air terminal devices. *Energy Buildings* **34**, 829–836.

Morawska, L. 2006 Droplet fate in indoor environments, or can we prevent the spread of infection? *Indoor Air* **16**, 335–347. (doi:10.1111/j.1600-0668.2006.00432.x)

Murphy, B. R., Chalhub, E. G., Nusinoff, S. R., Kasel, J. & Chanock, R. M. 1973 Temperature-sensitive mutants of influenza virus. 3. Further characterization of the ts-1 influenza A recombinant (H3N2) virus in man. *J. Infect. Dis.* **128**, 479–487.

Nicas, M. & Jones, R. M. 2009 Relative contributions of four exposure pathways to influenza infection risk. *Risk Anal.* **29**, 1292–1303. (doi:10.1111/j.1539-6924.2009.01253.x)

Nicas, M., Nazaroff, W. & Hubbard, A. 2005 Towards understanding the risk of secondary airborne infection: emission of respirable pathogens. *J. Occup. Environ. Hyg.* **2:3**, 143–154.

Riley, R. L. 1972 *Principles of UV air disinfection*. Public Health Service, 00-2215. Washington, DC: US Department of Health, Education and Welfare.

Riley, R. L., Permut, S. & Kaufman, J. E. 1971 Convection, air mixing, and ultraviolet air disinfection in rooms. *Arch. Environ. Health* **22**, 200–207.

Schaffer, F. L., Soergel, M. E. & Straube, D. C. 1976 Survival of airborne influenza virus: effects of propagating host, relative humidity, and composition of spray fluids. *Arch. Virol.* **51**, 263–273. (doi:10.1007/BF01317930)

Sze To, G. N., Wan, M. P., Chao, C. Y. H., Wei, F., Yu, S. C. T. & Kwan, J. K. C. 2008 A methodology for estimating airborne virus exposures in indoor environments using the spatial distribution of expiratory aerosols and virus viability characteristics. *Indoor Air* **18**, 425–438. (doi:10.1111/j.1600-0668.2008.00544.x)

Sze To, G. N., Wan, M. P., Chao, C. Y. H., Fang, L. & Melikov, A. 2009 Experimental study of dispersion and deposition of expiratory aerosols in aircraft cabins and impact on infectious disease transmission. *Aerosol Sci. Technol.* **43**, 466–485. (doi:10.1080/02786820902736658)

Tellier, R. 2006 Review of aerosol transmission of influenza A virus. *Emerg. Infect. Dis.* **12**, 1657–1662.

Wan, M. P. & Chao, C. Y. H. 2005 Effect of changing the air distribution system on the dispersion of droplet phase aerosols in an enclosure. In *Proc. 10th Int. Conf. on Indoor Air Quality and Climate, Beijing, China, 4–9 September 2005*, pp. 2696–2700.

Wan, M. P., Chao, C. Y. H., Ng, Y. D., Sze To, G. N. & Yu, W. C. 2007 Dispersion of expiratory aerosols in a general hospital ward with ceiling mixing type mechanical ventilation system. *Aerosol Sci. Technol.* **41**, 244–258. (doi:10.1080/02786820601146985)

Wan, M. P., Sze To, G. N., Chao, C. Y. H., Fang, L. & Melikov, A. 2009 Modeling the fate of expiratory aerosols and the associated infection risk in an aircraft cabin environment. *Aerosol Sci. Technol.* **43**, 322–343.

Wells, W. F. 1934 On air-borne infection. Study II. Droplets and droplet nuclei. *Am. J. Hyg.* **20**, 611–618.

Wells, W. F. 1955 *Airborne contagion and air hygiene*, pp. 117–122. Cambridge, MA: Cambridge University Press.

Xie, X., Li, Y., Chwang, A. T. Y., Ho, P. L. & Seto, W. H. 2007 How far droplets can move in indoor environments: revisiting the Wells evaporation-falling curve. *Indoor Air* **17**, 211–225. (doi:10.1111/j.1600-0668.2007.00469.x)

Xu, P., Kujundzic, E., Peccia, J., Millie, P. S., Moss, G., Hernandez, M. & Miller, S. L. 2005 Impact of environmental factors on efficacy of upper-room air ultraviolet germicidal irradiation for inactivating airborne mycobacteria. *Environ. Sci. Technol.* **39**, 9656–9664. (doi:10.1021/es0504892)

Yeager, H., Lacy, J., Smith, L. R. & LeMaistre, C. A. 1967 Quantitative studies of mycobacterial populations in sputum and saliva. *Am. Rev. Resp. Dis.* **95**, 998–1004.

Zhu, S., Kato, S., Murakami, S. & Hayashi, T. 2005 Study on inhalation region by means of CFD analysis and experiment. *Build. Environ.* **40**, 1329–1336. (doi:10.1016/j.buildenv.2004.11.009)

Zhu, S., Kato, S. & Yang, J. H. 2006 Study on transport characteristics of saliva droplets produced by coughing in a calm indoor environment. *Build. Environ.* **41**, 1691–1702. (doi:10.1016/j.buildenv.2005.06.024)